2019 IEEE International Ultrasonics Symposium (IUS)
Glasgow, Scotland, October 6-9, 2019

Block-wise Independent Component Analysis for Slow Flow Non-Contrast Ultrasound Imaging

Abbie Weeks
Department of Biomedical Engineering
Vanderbilt University
Nashville, TN, USA
abbie.e.weeks@vanderbilt.edu

Jaime Tierney
Department of Biomedical Engineering
Vanderbilt University
Nashville, TN, USA
jaime.e.tierney@vanderbilt.edu

Brett Byram
Department of Biomedical Engineering
Vanderbilt University
Nashville, TN, USA
brett.c.byram@vanderbilt.edu

***Abstract*—Slow blood flow imaging has proven to be a difficult clinical problem. Imaging modalities, such as MR Angiography and Contrast-Enhanced Ultrasound, attempting to solve this problem are expensive and time-consuming. Both eigen-based filters and spatial filters have been proposed to improve ultrasound power Doppler blood flow images. Block-wise methods and Independent Component Analysis (ICA) filters have each individually been previously shown to improve tissue clutter and noise suppression. Here, we aim to develop a Block-wise implementation of ICA to evaluate blood flow in ultrasound blood flow imaging. We show through phantom studies that by applying ICA in a block-wise manner, we see qualitative improvements as compared to other eigen-based filters applied in global and block-wise manners.**

Keywords—block-wise, independent component analysis, slow blood flow, power Doppler, ultrasound

I. Introduction

Robust and cost-effective slow blood flow imaging remains evasive within the medical imaging community. Both contrast-enhanced magnetic resonance angiography and contrast-enhanced computed tomography have been used analyze vasculature. However, MR angiography is time consuming and expensive, and thus cannot be repeated regularly on a single patient, and CT requires an injection of iodine-based contrast agents [1], [2] and contrast requirements have thus limited the utility of these modalities in both research and clinical practice[3].

Recently, improved blood filtering methods have been introduced for non-contrast power Doppler ultrasound blood flow imaging. These methods employ eigen-based filters often through Singular Value Decomposition (SVD) or Independent Component Analysis (ICA) [4]–[6]. Top Hat and Hessian filters have also been employed to augment these methods [7].

Independent Component Analysis (ICA) is a method for recovering independent source signals from a linearly-mixed dataset by analyzing the covariance of the data and maximizing statistical independence [8]. Unlike singular value decomposition, independent components need not be orthogonal, nor correspond to the direction of maximal variance [8], [9]. These properties theoretically make ICA more robust to separating overlapping signals such as those encountered with slow flow power Doppler ultrasound imaging [6].

Global methods of SVD and ICA must contend with highly non-stationary noise due to tissue movement throughout the image [5]. Dividing the data into blocks increases the stationarity of the noise within the local block, making separation of signals more complete and more robust at slow blood flows when tissue signal overwhelms blood signal [5]. Our goal is to develop a block-wise ICA algorithm to improve tissue, blood, and noise separation in power Doppler Ultrasound images.

II. Methods

A. Theory

Received ultrasound signal from in vivo blood flow consists of signals from tissue, blood, and noise. We are only interested in the blood signal; methods such as PCA/SVD and ICA allow us to separate the blood signal from that of the tissue and noise. PCA methods can only remove second-order dependencies between the three signal sources, assuming that the principal components are linearly uncorrelated both spatially and temporally [10]–[12]. ICA, however, can remove higher order dependencies, and assumes that the components of each signal are entirely independent [12]. Thus ICA should theoretically separate tissue, blood, and noise signals more effectively than PCA, and this has been shown to be true by Tierney, et al [6].

It has been shown previously that applying PCA in a block-wise fashion improves SNR and CNR of the filtered images [5]. Noise signal is more stationary within a small block of the dataset compared to the entire dataset, and is thus easier to separate [5]. We posit that applying ICA in a block-wise fashion will also improve delineation between tissue and blood in addition to noise separation.

B. Implementation

We begin with a beamformed power Doppler Ultrasound signal, s, that consists of tissue (c), blood (b), and noise (n) signals (Eq 1).

$$s(z,x,t) = c(z,x,t) + b(z,x,t) + n(z,x,t) \qquad (1)$$

978-1-7281-4596-9/19/$31.00 ©2019 IEEE

The signal s is 3-D, with dimensions *depth x beams x slow time* (*Z, X, t*). Signal *s* is separated into overlapping blocks of size *z x x x t*. The blocks overlap in the axial (depth) and lateral (beam) dimensions, but not the temporal dimension. The redundant overlapping of the blocks theoretically increases the SNR of the image. Each block is then operated on as a signal independent of surrounding blocks [5].

We can reshape s_{block} into a 2-D Casorati matrix S_{block} to perform PCA or ICA [5], [11]. S_{block} has dimensions $n = zx$ and $m = t$. As shown in Song, et al, PCA directly decomposes this Casorati matrix. ICA, alternatively, works by solving for two matrices, A and Y, whose product approximates the Casorati matrix, as shown in Eq 2[5].

$$S = AY \tag{2}$$

Our implementation of ICA, as described by Tierney, et al, operates on the transposed Casorati matrix with dimensions $m \times x \times n$ and only considers the real part of the signal [6]. Additionally, we only operate on the spatial eigenvectors of S_{block}, shown by Equations 3 and 4.

$$S = U\lambda V' \tag{3}$$

$$S_s = \lambda V' = AY \tag{4}$$

Most ICA algorithms work by solving for matrix A, and using A^{-1} and S to solve for Y. For our implementation, we use a maximum likelihood method with BFGS optimization to solve for A [13]–[15].

Once the independent components have been determined, each component must be classified as either tissue or blood. To do this we first take the Kurtosis of each independent component, then arrange those Kurtosis values in descending order. Next, we calculate the gradient along the descending Kurtosis values and empirically select a threshold. Kurtosis is the fourth moment about the mean , and describes the shape of a distribution with reference to the Gaussian Normal Distribution [16]. Blood flow has been shown to be more non-Gaussian than tissue clutter, and thus has greater Kurtosis [16]. Therefore, we discard components that fall below the threshold as tissue components, and retain those above as blood components.

As each block is operated upon, the filtered signal for that block is reshaped back to its original dimensions of $z \times x \times t$ and replaced in the appropriate position within the total dataset. To account for the overlapping of blocks, each pixel in the total filtered dataset is divided by the total number of blocks in which that pixel appeared such that the final value of any pixel in the total filtered dataset can be described by Equation 5 (variant on the Song equation):

$$s_{filtered}(z,x,t) = \frac{1}{N}\sum_{i=1}^{N} s_i(z,x,t) \tag{5}$$

where N is the total number of blocks in which a certain pixel from a certain block appears. A pixel from a particular block is denoted $s_i(z, x, t)$.

C. Single-Vessel Phantoms Experiment

Data from six single-vessel phantoms were used to evaluate the block-wise ICA algorithm. The phantoms were made of a polyvinyl alcohol and graphite mixture and contained a 600 µm diameter vessel in a 2 x 3 cm mold. A syringe pump was used to pump blood-mimicking fluid at rates of 1 mm/s and 5 mm/s through the phantoms. Five realizations of each flow speed were evaluated (4 phantoms were used for both flow speeds, 1 for 1 mm/s only, and 1 for 5 mm/s only). The data were collected with a hand-held Verasonics L12-5 probe using a Plane Wave sequence. The plane waves were acquired using a 7.8 MHz center frequency for 1 s with 9 evenly spaced angles from –8 to 8 at a PRF of 9 kHz. The channel data were beamformed using parallel receive beamforming. Synthetic transmit focusing was achieved by summing consecutive angles, resulting in a final PRF of 1 kHz. An F# of 2 was achieved during beamforming through Hann apodization and aperture growth. The final beamformed data were band-pass filtered and up-sampled by a factor of 2 resulting in a 62.5 MHz sampling frequency. [6].

Several block sizes were tested using phantom data. Similar to Song, et al, we tested blocks of equal size in both the axial and lateral dimensions (e.g. 40x40, 80x80, etc.). Additionally, we chose to expand our testing to blocks of unequal dimension, particularly increasing the block size in the axial dimension. The number of axial samples ranges from approximately 10 to 50 times more than the number of lateral samples for power Doppler ultrasound. Increasing the axial block size reduces the computational load, as fewer blocks are necessary and also helps to compensate for the sample disparity between the axial and lateral dimensions of the full dataset.

D. Image Quality Evaluation

To evaluate each image, Contrast-to-Noise Ratio (CNR), Signal-to-Noise Ratio (SNR), and Contrast Ratio (CR) were calculated as in [5], [10], [17].

III. Results and Discussion

We performed a comparison between global and block-wise SVD and ICA for both 1 mm/s and 5 mm/s flow speeds. Figs. 1 and 2 display those results for a selected phantom for each flow speed. There is notable increase in the visibility of the blood flow in the ICA case as opposed to the SVD case, and in the block-wise cases as opposed to the global cases. Table 1 provides SNR, CNR, and CR values averaged across five examples for the 5 mm/s flow speed.

While there is an improvement in the image metrics between global and block-wise methods, the metrics overall are objectively poor and do not reflect the observed qualitative improvements. There are several potential causes for the discrepancies between the qualitative and quantitative results. Block-wise ICA fails to reduce the variance of the background sufficiently; variations from block to block lead to inconsistencies in tissue clutter and noise suppression. Some of these variations stem from the empirically-chosen Kurtosis threshold. The number of independent components

chosen varies for each block based on the threshold, but that threshold is the same threshold for each block. A more adaptive or algorithmic choice of threshold could potentially improve the high background variation from block to block. Additionally, Kurtosis and non-Gaussianity may not be enough to differentiate between source signals; the addition of a threshold based on entropy or mutual information could also provide improvement.

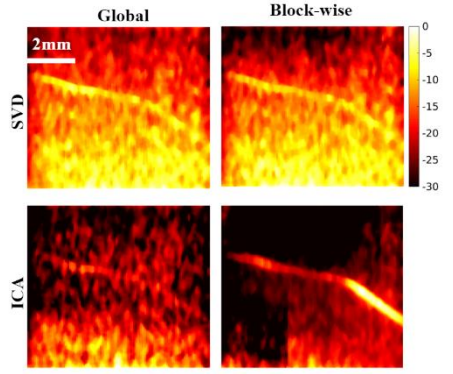

Fig. 1. **1 mm/s flow:** For both SVD and ICA, applying filters in a blockwise manner reduces noise and increases vessel visibiliy. The slower flow speed contributes to lesser blood signal, causing a blocking artifact to be visible in the Block-wise ICA realization. Block-wise methods implemented with 200x80 pixel blocks.

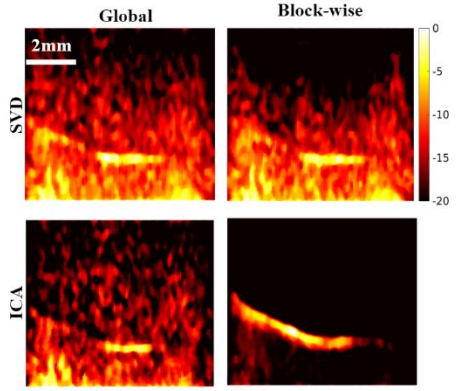

Fig. 2. **5 mm/s flow:** For both SVD and ICA, applying filters in a blockwise manner reduces noise and increases vessel visibiliy. Higher blood signal from higher flow speed results in less blocking artifact in the Block-wise ICA realization. Block-wise methods implemented with 200x80 pixel blocks.

TABLE I. IMAGE QUALITY METRICS

	Global SVD	***Global ICA***	***Block-wise SVD***	***Block-wise ICA***
CNR	14.75 ± 1.79	13.91 ±3.25	15.41 ± 3.94	16.22 ± 4.81
CR	1.56 ± 0.56	2.01 ± 1.07	1.82 ±1.21	1.20 ± 0.66
SNR	0.79 ± 0.25	2.02 ± 1.36	1.37 ± 0.54	1.19 ± 0.67

IV. CONCLUSION

Slow blood flow imaging still remains an obstacle clinically. Proposed imaging modality solutions are expensive and time consuming. Eigen-based and spatial filters have been proposed with limited success. Here, we have proposed Block-wise Independent Component Analysis as a filtering method for slow blood flow imaging of non-contrast ultrasound power Doppler images.

ACKNOWLEDGMENT

The authors would like to thank the Staff of the Vanderbilt University ACCRE Computing Resource. This work was supported by NSF ISS-1750994.

REFERENCES

[1] R. J. Lewandowski *et al.*, "A Comparison of Chemoembolization Endpoints Using Angiographic versus Transcatheter Intraarterial Perfusion/MR Imaging Monitoring," *J. Vasc. Interv. Radiol.*, vol. 18, pp. 1249–1257, 2007.

[2] D. B. Hasdemir *et al.*, "Evaluation of CT vascularization patterns for survival prognosis in patients with hepatocellular carcinoma treated by conventional TACE," *Diagnstoic Interv. Radiol.*, vol. 23, no. 3, pp. 217–222, 2017.

[3] M. Bruce, M. Averkiou, K. Tiemann, S. Lohmaier, J. Powers, and K. Beach, "Vascular flow and perfusion imaging with ultrasound contrast agents," *Ultrasound Med. Biol.*, vol. 30, no. 6, pp. 735–743, Jun. 2004.

[4] A. Yu and L. Lovstakken, "Eigen-based clutter filter design for ultrasound color flow imaging: a review," *IEEE Trans. Ultrason. Ferroelectr. Freq. Control*, vol. 57, no. 5, pp. 1096–1111, May 2010.

[5] P. Song, A. Manduca, J. D. Trzasko, and S. Chen, "Ultrasound Small Vessel Imaging With Block-Wise Adaptive Local Clutter Filtering," *IEEE Trans. Med. Imaging*, vol. 36, no. 1, pp. 251–262, Jan. 2017.

[6] J. E. Tierney, D. M. Wilkes, and B. C. Byram, "Independent component analysis-based tissue clutter filtering for plane wave perfusion ultrasound imaging," in *Medical Imaging 2019: Ultrasonic Imaging and Tomography*, 2019, vol. 10955, p. 2.

[7] M. Bayat, M. Fatemi, and A. Alizad, "Background Removal and Vessel Filtering of Noncontrast Ultrasound Images of Microvasculature," *IEEE Trans. Biomed. Eng.*, vol. 66, no. 3, pp. 831–842, Mar. 2019.

[8] J. Shlens, "A Tutorial on Independent Component Analysis."

[9] J. Shlens, "A Tutorial on Principal Component Analysis."

[10] J. Baranger, B. Arnal, F. Perren, O. Baud, M. Tanter, and C. Demene, "Adaptive Spatiotemporal SVD Clutter Filtering for Ultrafast Doppler Imaging Using Similarity of Spatial Singular Vectors," *IEEE Trans. Med. Imaging*, vol. 37, no. 7, pp. 1574–1586, Jul. 2018.

[11] C. Demene *et al.*, "Spatiotemporal Clutter Filtering of Ultrafast Ultrasound Data Highly Increases Doppler and fUltrasound Sensitivity," *IEEE Trans. Med. Imaging*, vol. 34, no. 11, pp. 2271–2285, Nov. 2015.

[12] C. M. Gallippi and G. E. Trahey, "Adaptive Clutter Filtering via Blind Source Separation for Two-Dimensional Ultrasonic Blood Velocity Measurement," *Ultrason. Imaging*, vol. 24, no. 4, pp. 193–214, Oct. 2002.

[13] A. J. Bell and T. J. Sejnowski, "An information-maximisation approach t o blind separation and blind deconvolution."

[14] L. K. Hansen, J. Larsen, and T. Kolenda, "Blind detection of independent dynamic components," in *2001 IEEE International Conference on Acoustics, Speech, and Signal Processing. Proceedings (Cat. No.01CH37221)*, vol. 5, pp. 3197–3200.

[15] H. B. Nielsen, "UCMINF-AN ALGORITHM FOR UNCONSTRAINED, NONLINEAR OPTIMIZATION," 2000.

[16] G. Cloutier, M. Daronatand, D. Savéry, D. Garcia, L.-G. Durand, and F. S. Foster, "Non-Gaussian statistics and temporal variations of the ultrasound signal backscattered by blood at frequencies between 10 and 58 MHz.," *J. Acoust. Soc. Am.*, vol. 116, no. 1, pp. 566–77, Jul. 2004.

[17] Y. L. Li, D. Hyun, L. Abou-Elkacem, J. K. Willmann, and J. J. Dahl, "Visualization of Small-Diameter Vessels by Reduction of Incoherent Reverberation with Coherent Flow Power Doppler," *IEEE Trans. Ultrason. Ferroelectr. Freq. Control*, vol. 63, no. 11, pp. 1878–1889, Nov. 2016.